

indiqué sur la Fig. 6. En réalité cet ensemble ne forme pas une unité chimique, caractérisée par des liaisons intermoléculaires; le choix d'une unité asymétrique chimiquement définie est lié à la connaissance de la disposition des atomes d'hydrogène, discutées ci-dessous. De même, pour justifier la formation de macule, et le désordre, on peut admettre que l'édifice cristallin puisse adopter plusieurs configurations, peu différentes entr'elles, en rapport avec l'emplacement des atomes d'hydrogène.

Nous avons essayé de déterminer les positions des hydrogènes par la considération des plus courtes distances intermoléculaires, indiquées sur la Fig. 6. On voit qu'il est impossible de localiser des liaisons hydrogène, caractérisées par des distances particulièrement courtes, puisque toutes les distances sont au moins égales au contact de van der Waals. D'autre part l'observation détaillée de la structure suggère plusieurs dispositions possibles des atomes d'hydrogène. Avant d'essayer d'élucider cette question, nous préférons attendre les résultats des études actuellement en cours sur la structure cristalline de  $\text{HNO}_3 \cdot \text{H}_2\text{O}$  et de  $\text{HNO}_3 \cdot 3\text{H}_2\text{O}$ , ainsi que l'interprétation des spectres Raman des acides nitriques cristallins.

La disposition des molécules, telle qu'on peut voir sur la Fig. 6, tend à opposer les radicaux  $\text{NO}_2$  aux radicaux  $\text{OH}$ . En particulier, la disposition des molécules autour de l'axe hélicoïdal est caractéristique d'un enchaînement de dipôles, telle que l'on trouve très

souvent dans les cristaux organiques. Toutes les molécules adoptent cet enchaînement de dipôles, sauf celles immédiatement voisines des centres de symétrie (Fig. 6). En effet, quand on trouve une suite de deux éléments différents  $A$  et  $B$ , les molécules situées à la frontière de ces éléments opposent leurs radicaux  $\text{OH}$ , contrairement à toutes les autres molécules du cristal, tandis qu'à la frontière de deux éléments  $A-A$  (ou  $B-B$ ) ces mêmes molécules opposent les radicaux  $\text{OH}$  aux  $\text{NO}_2$  (Fig. 8). Cette remarque pourrait suggérer une justification à l'apparition du désordre.

### Références

- BAUER, E. & MAGAT, M. (1944). *Mémor. Serv. Chim. État*, **31**, 171.  
 BOUTTIER, L. (1949). *C.R. Acad. Sci., Paris*, **228**, 1419.  
 CHEDIN, J. (1939). *J. Phys. Radium*, **10**, 445.  
 DALMON, R. & FREYMAN, R. (1940). *C.R. Acad. Sci., Paris*, **211**, 472.  
 GRISON, E., ERIKS, K. & VRIES, J. L. DE (1950). *Acta Cryst.* **3**, 290.  
 GUINIER, A. & GRIFFOUL, R. (1948). *Acta Cryst.* **1**, 188.  
 HENDRICKS, S. B. (1940). *Phys. Rev.* **57**, 443.  
 HENDRICKS, S. B. & JEFFERSON, M. E. (1939). *Amer. Min.* **24**, 729.  
 LUZZATI, V. (1950). *C.R. Acad. Sci., Paris*, **230**, 101.  
 MAXWELL, L. R. & MOSLEY, V. M. (1940). *J. Chem. Phys.* **8**, 735.  
 ROBINSON, K. & BRINDLEY, G. W. (1949). *Proc. Leeds Phil. Lit. Soc.* **5**, 102.

*Acta Cryst.* (1951). **4**, 131

## The Crystal Structure of Hydrate Racemic Acid

BY G. S. PARRY\*

*Birkbeck College Research Laboratory (University of London), 21 Torrington Square, London W.C. 1, England*

(Received 14 June 1950)

The crystals are triclinic with  $a=8.06$ ,  $b=9.60$ ,  $c=4.85$  Å.;  $\alpha=70.4^\circ$ ,  $\beta=97.2^\circ$ ,  $\gamma=112.5^\circ$ . The cell has a centre of symmetry and contains one *d*- and one *l*-tartaric acid molecule and also two water molecules. Atomic parameters have been obtained and refined by two-dimensional electron-density summations. Some phase relations obtained from Harker-Kasper inequalities helped to determine the  $z$  parameters. The configuration of the tartaric acid molecule agrees with that found in Rochelle salt and in tartaric acid. The structure is held together by an extensive arrangement of hydrogen bonds, all of which form closed systems. Columns are formed parallel to the  $c$  axis by square hydrogen-bond systems involving the hydroxyl groups. Hydrogen bonds between carboxyl groups hold these columns together in sheets parallel to  $(1\bar{1}0)$ , and these sheets are held together by the water molecules. Difficulties arise in the precise location of the hydrogen bonds to the water molecules owing to the close approach of many oxygen atoms. A plane arrangement is favoured although other possibilities exist.

### Introduction

Racemic acid is one of the optically inactive forms of tartaric acid and was shown by Pasteur (1848) to consist in equal quantities of two acids, one of which was

\* Now at Department of Chemistry, The University, Leeds 2, England.

identical with the naturally occurring tartaric acid. The other had the same chemical properties as natural tartaric acid but had opposite sign for the specific rotation of a beam of plane polarized light. Hence both crystals and solutions of the acid are optically inactive. Racemic acid is a compound and not merely a mixture of the

two forms of tartaric acid. Its melting-point (206° C.) is appreciably higher than that of tartaric acid (170° C.), and there are also considerable differences in aqueous solubility. The heat of combustion of anhydrous racemic acid is slightly greater (2.3 kcal./mole) than that of tartaric acid, indicating some weak chemical interaction between the two stereoisomers.

### Preliminary investigation

The acid crystallizes from aqueous solution at normal temperatures with one molecule of water for each tartaric acid molecule. An anhydrous form of the acid is obtained from aqueous solution if crystallization takes place above 70° C. Morphological examinations (Groth, 1906–19) have shown that crystals of both forms are triclinic and possess a centre of symmetry. The first X-ray investigation was made by Astbury (1923) who examined the anhydrous acid and postulated a structure for the acid which was consistent with the observed physical properties. Although this structure is now of little value, the present work has confirmed his conclusion that racemic acid does not occur in the crystalline state as a double molecule of the two forms

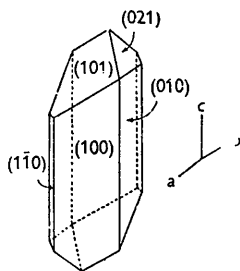


Fig. 1.

Fig. 1. Clinographic projection of a crystal of hydrate racemic acid.

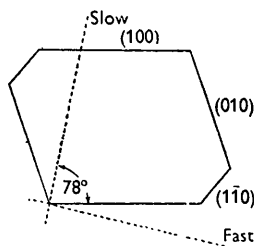


Fig. 2.

Fig. 2. Orientation of the extinction directions in a crystal section cut normal to the *c* axis. The molecule was assumed to lie close to the direction of the greater refractive index.

of tartaric acid. Further X-ray work on both crystalline modifications of the acid by Gerstacker, Moller & Reis (1927) was limited to a determination of the cell constants. Single crystals of the anhydrous acid are difficult to obtain, the usual result of aqueous crystallization being a polycrystalline mass formed by multiple twinning. For this reason the present work was done on the hydrate form of the acid. When grown from aqueous solution, well-formed prismatic crystals with the development shown in Fig. 1 were obtained.

A short optical examination gave results in agreement with those of previous investigators (Groth, 1906–19), although no accurate measurements were attempted. Goniometrical observations were made in order to identify the axes chosen by previous investigators. The dimensions of the real and reciprocal cells were obtained from oscillation photographs, and the reciprocal-cell angles were found from Weissenberg

photographs and goniometrical measurements. The real cell angles were then found from relations of the type

$$\sin \gamma = \frac{c d_{100} d_{010}}{ab d_{001} \sin \gamma^*}$$

This relation is not very satisfactory if the cell angle is near 90°, for small errors in the measured quantities can make an appreciable difference in the calculated angle. It was thought desirable to check the values so obtained by recalculating the reciprocal cell angles, using expressions of the type

$$\cot \frac{1}{2}\alpha^* = \frac{\sin(\sigma - \beta) \sin(\sigma - \gamma)}{\sin \sigma \sin(\sigma - \alpha)}, \quad \text{where } \sigma = \frac{1}{2}(\alpha + \beta + \gamma)$$

With the values of cell parameters finally chosen, the reciprocal-cell angles calculated in this way did not differ from those used initially by more than  $\pm 20'$ . Finally, the cell angles were calculated solely from goniometrical data, and the results did not differ from the X-ray determinations by more than 20'. A summary of the cell constants is given in Table 1. This cell differs from that defined by morphological studies alone in that a new direction has been chosen for the *b* axis.

Table 1. Cell constants of hydrate racemic acid

$a = 8.06_0$ A.	$d_{100} = 7.46_7$ A.		
$b = 9.60_7$ A.	$d_{010} = 8.37_6$ A.		
$c = 4.85_4$ A.	$d_{001} = 4.57_8$ A.		
$\alpha = 70^\circ 23' \dagger$	$70^\circ 04' \ddagger$	$\alpha^* = 108^\circ 40' \dagger$	$108^\circ 54' \ddagger$
$\beta = 97^\circ 12'$	$97^\circ 06'$	$\beta^* = 90^\circ 46'$	$90^\circ 36'$
$\gamma = 112^\circ 28'$	$112^\circ 08'$	$\gamma^* = 68^\circ 50'$	$69^\circ 01'$

† Determined from X-ray measurements.

‡ Determined from goniometrical measurements.

This alteration was made in order that all the atoms from any tartaric acid molecule should lie within the chosen unit cell. The cell is therefore significant from a structural point of view. The face indices on these new axes are not in general as simple as on the original axes. One exception is the important prismatic face now indexed as (100) which was previously indexed as (110). The equations transforming indices from the old to the new axes are:

$$h' = h, \quad k' = -(h + k - l), \quad l' = l,$$

where  $hkl$  are the original indices and  $h'k'l'$  the new indices.

The measured crystal density is  $1.700 \pm 0.003$  g.cm.<sup>-3</sup>, so that the cell contains one molecule of formula  $l\text{-C}_4\text{H}_6\text{O}_6 \cdot d\text{-C}_4\text{H}_6\text{O}_6 \cdot 2\text{H}_2\text{O}$  (calculated 0.999<sub>6</sub>).

Weissenberg photographs about the three main axes were used to collect the  $hkl$ ,  $h0l$  and  $0kl$  intensities, which were all estimated visually. The Lorentz polarization factor was derived by the method of Goldschmidt & Pitt (1948).

### The *c*-axis projection

An optical examination of a section cut perpendicular to the *c* axis gave the results shown in Fig. 2. The greatest refractive index made an angle of 78° with the

*b* axis so that it was oriented approximately parallel to  $(1\bar{2}0)$ .  $(010)$  and  $(1\bar{2}0)$  were perfect cleavages and the intensities of the X-ray reflexions from  $020$  and  $1\bar{2}0$  were very great. It therefore appeared probable that the tartaric acid molecules lay parallel to  $1\bar{2}0$ , being separated from each other in the *b* direction by about half the *b* axis (4.80 Å).

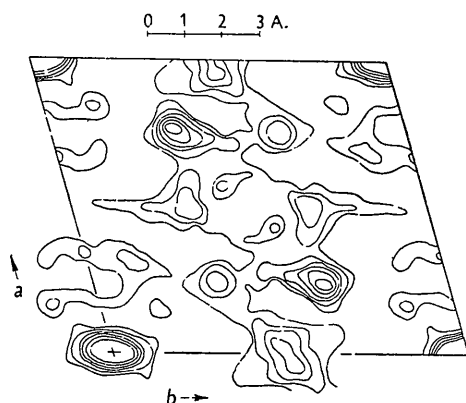


Fig. 3. Patterson projection on  $(001)$ . Contours at arbitrary intervals.

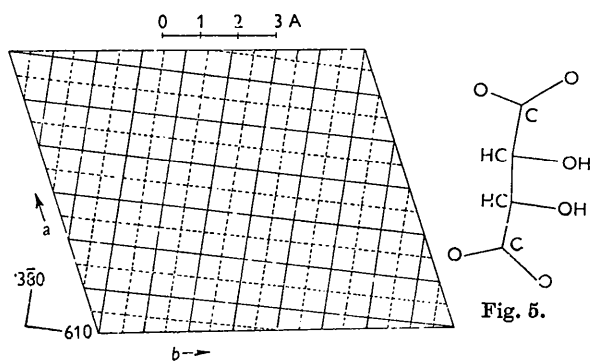


Fig. 4.

Fig. 4. Structure-factor graphs for 610 and  $3\bar{8}0$ . Full lines indicate maximum positive values, broken lines maximum negative values.

Fig. 5. Projection of the Beever-Hughes model of the tartaric acid molecule which would account for the structure-factor graphs shown in Fig. 4.

The Patterson projection perpendicular to the *c* axis (Fig. 3) showed a pronounced ridge of peaks lying about the line  $y = \frac{1}{2}$  in addition to a peak at  $(0, \frac{1}{2})$ . This was taken to support the general molecular arrangement suggested above, although a detailed interpretation of the peaks was not possible. An examination of the observed reflexions showed that two, 610 and  $3\bar{8}0$ , had very large geometrical structure factors. Graphs of these planes formed almost a square grid of side 1.2 Å. (Fig. 4). Assuming that the tartaric acid molecule had the same configuration as that found in Rochelle salt (Beever & Hughes, 1941) and in *d*-tartaric acid (Beever & Stern, 1948), then there was only one projection of the molecule (Fig. 5) which would account for this structure-factor grid. Trial

structure-factor calculations were made, placing this projection of the tartaric acid molecule at various positions in the unit cell. It was decided to include the contribution of the water molecule in these calculations in order that the agreement between the observed and calculated structure factors could be assessed. It was assumed that the water molecule would be found in the vicinity of one carboxyl group and was so placed that reasonable agreement between  $F$  (obs.) and  $F$  (calc.) was obtained from low-order planes that were not sensitive to the contribution of the tartaric acid molecule.

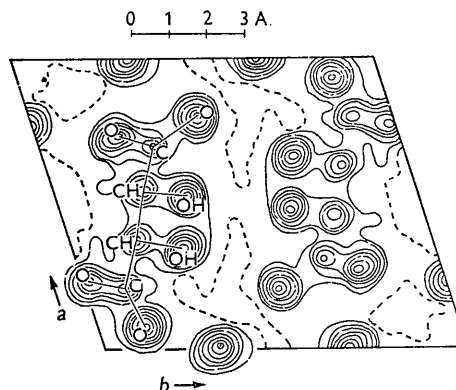


Fig. 6. Electron-density projection on  $(001)$ . Contours at intervals of  $1 \text{ e.A.}^{-2}$ , the first being broken.

After several attempts, a set of parameters was obtained which gave reasonable agreement between  $F$  (obs.) and  $F$  (calc.). The electron-density projection calculated from the predicted phases enabled  $x$  and  $y$  parameters for nine out of the eleven atoms to be estimated from resolved peaks. These parameters were then refined by successive Fourier summations until there were no further phase changes. During the course of the refinement, partial resolution of all atoms was obtained (Fig. 6) so that each of the final  $x$  and  $y$  parameters could be estimated from a Fourier peak.

#### The *b*- and *c*-axis projections

Harker & Kasper (1948) have derived the following inequality:

$$(U_H \pm U_{H'})^2 \leq (1 \pm U_{H+H'}) (1 \pm U_{H-H'}),$$

where

$$H = hkl,$$

$$U_H = F_{hkl}/Zf,$$

$f$  is the atomic scattering factor, and

$Z$  is the number of electrons in the unit cell.

By the use of this inequality, the following phase relations were obtained for some  $h0l$  reflexions:

$$[50\bar{2}] = [10\bar{2}] \quad [70\bar{1}] = [80\bar{1}] \quad [90\bar{1}].$$

From an examination of the structure-factor graphs for these planes and a knowledge of the expected projection of the tartaric acid molecule, it was found reasonable to suppose that all the phases would be positive. This in turn suggested that the water molecule

would be found close to the origin, and a trial calculation of the electron-density projection using most of the observed structure factors confirmed this. Once the position of the molecule had been established, simultaneous refinements of the  $a$ - and  $b$ -axis projections were made. When the refinement was complete, estimates of the  $z$  parameters for nine atoms had been obtained from Fourier peaks. Only two carbon atoms were unresolved on either projection (Figs. 7, 8).

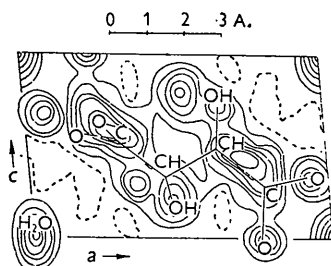


Fig. 7. Electron-density projection on (010). Contours at intervals of  $2 \text{ e.Å.}^{-2}$ , the first being broken.

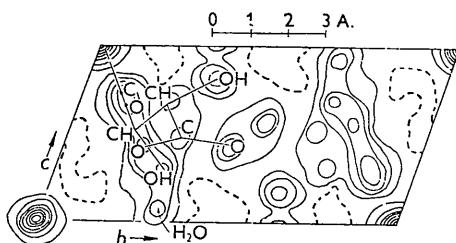


Fig. 8. Electron-density projection on (100). Contours at intervals of  $2 \text{ e.Å.}^{-2}$ , the first being broken.

### Corrections for extinction

It was clear from a comparison of the final values of the observed and calculated structure factors that the

majority of strong planes suffered from extinction. Summing only over planes having an observed intensity greater than 1000, it was found that  $\Sigma F(\text{obs.}) = 194$ , whereas  $\Sigma F(\text{calc.}) = 264$ . It had been anticipated that this crystal would show extinction effects, but an attempt to make the crystal texture an ideal mosaic by immersion in liquid air did not succeed. As some of these extinguished planes were adding considerably to the disagreement, a rough correction was attempted. It was assumed that the calculated structure factor was close to the correct value and that the effect of extinction could be represented by the equation

$$I(\text{calc.}) = I(\text{obs.}) e^{kI(\text{obs.})},$$

$$\text{so that } \log_e \frac{F(\text{calc.})}{F(\text{obs.})} = k I(\text{obs.}).$$

Values of  $k$  obtained from the extinguished planes varied from 2 to 5. As the correction applied was only small, a mean value of 3.3 was chosen. Values of the disagreement factor

$$\frac{\Sigma ||F(\text{obs.})| - |F(\text{calc.})||}{\Sigma |F(\text{obs.})|}$$

before and after correction are shown in Table 2. All the electron-density projections shown were computed using corrected values of the observed structure factors. Values of the observed and calculated structure factors for the three principal zones are given in Table 3.

Table 2. Disagreement factors before and after the correction for extinction

Zone	Before correction	After correction
$hk0$	0.213	0.191
$h0l$	0.248	0.226
$0kl$	0.274	0.265

Table 3. Observed and calculated structure factors

(1) $hk0$ zone			
$F(\text{obs.})$	$F(\text{calc.})$	$F(\text{obs.})$	$F(\text{calc.})$
100	9.6	140	14.6
200	7.7	150	< 0.8
300	7.9	160	1.8
400	18.6	170	5.3
500	2.0	180	4.6
600	3.4	190	3.3
700	6.6	1.10.0	0.9
800	1.3	210	12.3
900	1.8	220	18.4
010	1.3	230	2.0
020	20.8	240	14.0
030	10.3	250	< 0.9
040	0.9	260	1.3
050	6.3	270	3.7
060	7.7	280	3.6
070	< 1	290	4.0
080	< 1	310	9.2
090	5.3	320	19.3
0.10.0	0.9	330	5.6
110	9.6	340	7.0
120	2.3	350	3.0
130	11.4	360	5.9
		370	< 1
		380	3.2
		390	0.9
		410	7.9
		420	4.6
		430	4.7
		440	4.6
		450	2.3
		460	2.9
		470	1.5
		480	1.8
		510	9.8
		520	2.9
		530	8.4
		540	< 1
		550	2.4
		560	0.9
		570	1.8
		610	18.2
		620	9.8
		630	6.2



Table 3 (cont.)

			(3) <i>h</i> 0 <i>l</i> zone					
	<i>F</i> (obs.)	<i>F</i> (calc.)	<i>F</i> (obs.)	<i>F</i> (calc.)		<i>F</i> (obs.)	<i>F</i> (calc.)	
101	30.0	+23.3	104	6.5	-7.3	50 $\bar{2}$	13.9	+8.5
201	38.7	+34.8	204	0.7	-0.8	60 $\bar{2}$	1.6	-0.1
301	19.6	-14.6	304	1.3	+4.5	70 $\bar{2}$	1.8	+2.1
401	11.3	+8.1	404	<1	-1.2	80 $\bar{2}$	2.7	+2.2
501	9.8	+10.3	504	3.0	+4.1			
601	4.6	+6.8	604	1.6	+1.8	10 $\bar{3}$	2.3	-2.2
701	1.6	-1.2	704	1.2	-1.5	20 $\bar{3}$	3.1	+5.6
801	4.9	+6.6				30 $\bar{3}$	3.4	+2.3
901	0.5	+0.2	105	2.0	+3.0	40 $\bar{3}$	<1	-2.6
			205	1.8	-1.6	50 $\bar{3}$	0.8	+1.0
102	3.9	-3.8	305	3.3	-6.9	60 $\bar{3}$	1.8	-1.9
202	16.0	-17.9	405	2.0	+0.8	70 $\bar{3}$	2.0	-2.0
302	9.3	+11.3	505	<0.6	+0.5	80 $\bar{3}$	<0.2	+0.1
402	0.9	+0.7						
502	<0.9	+0.5	10 $\bar{1}$	2.1	+2.4	10 $\bar{4}$	1.2	+2.9
60 $\bar{2}$	2.3	-2.0	20 $\bar{1}$	2.4	+1.9	20 $\bar{4}$	9.2	-8.5
70 $\bar{2}$	2.7	+3.3	30 $\bar{1}$	4.1	+2.8	30 $\bar{4}$	3.2	-2.3
80 $\bar{2}$	1.3	+1.6	40 $\bar{1}$	4.1	+4.2	40 $\bar{4}$	<0.9	-0.7
90 $\bar{2}$	0.9	+2.2	50 $\bar{1}$	2.1	+1.5	50 $\bar{4}$	1.3	-0.1
			60 $\bar{1}$	5.2	-5.2	60 $\bar{4}$	<0.6	+1.0
103	15.2	+15.8	70 $\bar{1}$	5.6	+5.2			
203	6.6	-4.3	80 $\bar{1}$	0.8	+1.2	10 $\bar{5}$	1.8	-3.5
303	1.3	-2.9	90 $\bar{1}$	5.5	+5.2	20 $\bar{5}$	0.8	-1.4
403	5.6	+4.7				30 $\bar{5}$	2.0	-1.5
503	2.0	+1.8	10 $\bar{2}$	22.6	+17.6	40 $\bar{5}$	5.9	+3.6
603	2.6	-4.4	20 $\bar{2}$	7.5	-7.8			
703	<0.9	+0.4	30 $\bar{2}$	5.2	+4.5			
803	1.0	-1.2	40 $\bar{2}$	5.4	+5.1			

### Discussion of results

#### (i) *The tartaric acid molecule*

This has essentially the same configuration as in *d*-tartaric acid and Rochelle salt. Within the limits of error the carbon chain is planar and each half of the molecule, HCOH-COOH, also planar. The agreement between equivalent bond lengths determined in each half of the molecule is not good, but mean values should be more reliable and the shortening of the C-C bonds at the end of the chain may be significant (Fig. 9).

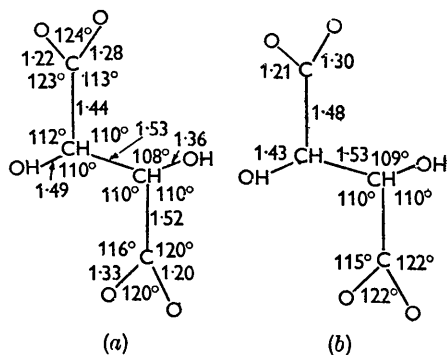


Fig. 9. The tartaric acid molecule showing (a) the observed dimensions, (b) the mean dimensions.

Much of the variation in the length of equivalent bonds is thought to be due to errors in the positions of the carbon atoms, for equivalent O-O distances in each half of the molecule agree to 0.01 Å.

There does appear to be a difference in the two C-O distances of both carboxyl groups and also a distortion of the carbon bond angles from a truly

trigonal arrangement. Although the differences in the C-O bond lengths are not outside the possible experimental error, these results agree closely with those of Morrison & Robertson (1949) for the saturated dicarboxylic acids (Table 4).

Table 4. *The dimensions of the carboxyl group*

Acid	C-O (1)	C-O (2)	$\theta$ (0)	$\theta$ (1)	$\theta$ (2)
$\beta$ -Succinic	1.25 Å.	1.30 Å.	122°	114°	124°
Adipic	1.23 Å.	1.29 Å.	126°	114°	120°
Sebacic	1.24 Å.	1.27 Å.	124°	116°	120°
$\beta$ -Glutaric	1.23 Å.	1.30 Å.	122°	115°	123°
Mean values	1.24 Å.	1.29 Å.	123°	115°	122°
Racemic hydrate (1)	1.22 Å.	1.28 Å.	120°	116°	120°
(2)	1.20 Å.	1.33 Å.	124°	113°	123°
Mean values	1.21 Å.	1.30 Å.	122°	115°	122°

In all these measurements, the probable error is such as to make the reality of the difference doubtful in any particular case. However, in view of the agreement between these several determinations, the difference is probably real. It is reasonable to suppose that the shorter of the two bonds represents the C=O. If this is so, then it is the oxygen of each carboxyl group which is adjacent to the hydroxyl in that half of the molecule. The distance between these two atoms is only 2.65 Å., and the explanation of this must be associated with the planarity of the HCOH-COOH grouping.

#### (2) *The structural arrangement of the d- and l-tartaric acid molecules*

Each tartaric acid molecule forms hydrogen bonds to other tartaric acid molecules of both the same and the opposite stereochemical configuration, and also to

water molecules. The hydrogen bonds formed only between the tartaric acid molecules belong to two independent systems:

(i) A square system of hydrogen bonds formed from the hydroxyl groups. Each hydroxyl forms two hydrogen bonds to other hydroxyls, one being on a *d*- and the other on an *l*-molecule so that the 'square' is formed from hydroxyls on four molecules. The system is grouped around a centre of symmetry and is necessarily planar. The two independent sides have lengths 2.75 and 2.83 Å., while the angle between them is 91°.

(ii) Hydrogen bonds formed between two carboxyl groups which are related by a centre of symmetry. These bonds unite one *d*- and one *l*-molecule. The length of the hydrogen bond formed is 2.72 Å.

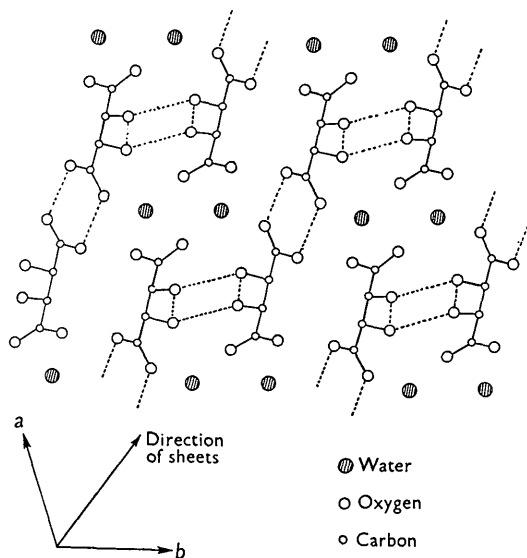


Fig. 10. The structure viewed normal to the *c* axis. The drawing shows the two principal intermolecular hydrogen-bonding systems, the squares forming columns of molecules parallel to the *c* axis, and the carboxyl groups linking these columns together to form sheets.

The first of these holds the *d*- and *l*-molecules together in columns which run parallel to the *c* axis, while the second unites these columns to form sheets which lie parallel to (110) (see Fig. 10). These sheets are in turn held together by the water molecules which form hydrogen bonds to the second carboxyl group of each tartaric acid molecule. Although the function of the water molecule in the structure is clear, attempts to assign a system of hydrogen bonds to it have met with difficulty.

In organic structures containing a relatively small number of hydrogen-bonding groups it has proved easy to identify in the structure the position of the hydrogen bonds formed. For instance, if a hydrogen bond is formed between two hydroxyl groups, the distance between the oxygen atoms would be 2.7–2.9 Å., whereas if no bond is formed, the distance would be

greater than 3.2 Å. In the case of racemic acid the number of hydrogen-bonding groups is large, the tartaric acid molecule rigid, and the structure very compact. It might be expected, therefore, that some non-bonded atoms could approach closer than the accepted van der Waals distance, and also that hydrogen-bond distances might be found somewhat larger than the normally accepted values. The difficulty then is to decide whether or not an interatomic distance of 2.9–3.1 Å. is due to hydrogen-bond formation. This difficulty could obviously be avoided simply by noting the occurrence of these short distances without attempting an interpretation of them. It was felt worth while, however, to see how far the known characteristics of hydrogen-bond formations could be used in addition to the length criterion to provide a set of 'hydrogen bonds' to the water molecule.

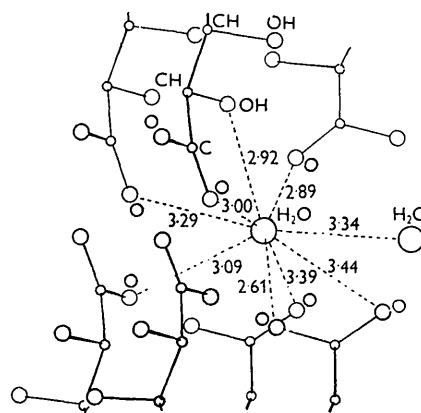


Fig. 11. The environment of a water molecule.

There were altogether five oxygen atoms at distances of less than 3.10 Å. from the water molecule (Fig. 11), although a tetrahedral arrangement of hydrogen bonds was not possible. It was considered significant that four out of these five atoms were grouped approximately in a plane. One of these four was situated at the corner of the hydrogen-bond square previously referred to, and it was considered unlikely that it would form further bonds. It was therefore supposed that hydrogen bonds would be formed between the water molecule and the three remaining atoms. The three hydrogen bonds have lengths 2.61, 2.89 and 3.00 Å.; they are almost coplanar but are not arranged trigonally.

Two of these hydrogen bonds form part of another hydrogen-bond system, a parallelogram having two short sides (2.61 and 2.72 Å.) and two long sides (3.00 and 3.05 Å.). This parallelogram is in the same plane as the three bonds to the water molecule, and when inverted across the centre of symmetry forms an extensive plane array (Figs. 12, 13). There are two difficulties with this arrangement. The first is that if all the hydrogen bonds in the plane are real then there are not sufficient hydrogen atoms. (This difficulty would

not arise if the 3.05 Å. distance were not a hydrogen bond but simply a close van der Waals approach.) The second difficulty is the small angle required between some hydrogen bonds ( $67^\circ$  and  $70^\circ$ ). It is possible that

It is possible, therefore, that split hydrogen bonds may occur here, although in view of the alternative explanation of the first difficulty this can only be a tentative suggestion.

This work forms part of an approved Thesis for Ph.D. in London University. I would like to thank Dr C. H. Carlisle and Dr G. J. Pitt (who suggested the form of the extinction correction) for some helpful discussions at various stages in the work. I am indebted to the Department of Scientific and Industrial Research for a maintenance allowance.

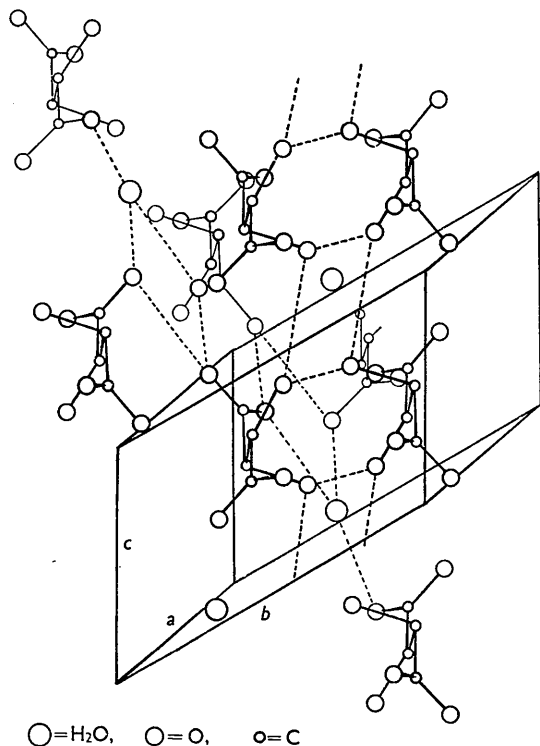


Fig. 12. A drawing of the structure. The broken lines represent the proposed hydrogen bonds.

these two difficulties are related. In the structure of glycine, Albrecht & Corey (1939) have proposed that 'split' hydrogen bonds can be formed, so that one hydrogen atom can cause the close approach of more than one oxygen atom. The angle between these bonds is  $69^\circ$ , close to the small angle found in racemic acid.

*Acta Cryst.* (1951). 4, 138

### Interatomic Distances in $\text{Co}_2\text{Al}_9$ \*

BY LINUS PAULING

*Gates and Crellin Laboratories of Chemistry, California Institute of Technology, Pasadena, California, U.S.A.*

(Received 15 August 1950)

It is pointed out that the system of metallic radii leads to interatomic distances in good agreement with those observed for the compound  $\text{Co}_2\text{Al}_9$ .

In a recent paper Mrs A. M. B. Douglas (1950) has reported the results of her careful determination of the

structure of the intermetallic compound  $\text{Co}_2\text{Al}_9$ . In this compound each cobalt atom is surrounded by nine aluminum atoms, at the average distance  $2.47_0$  Å. Mrs Douglas, in her paper, stated that 'Corrections

\* Contribution No. 1448 from the Gates and Crellin Laboratories.

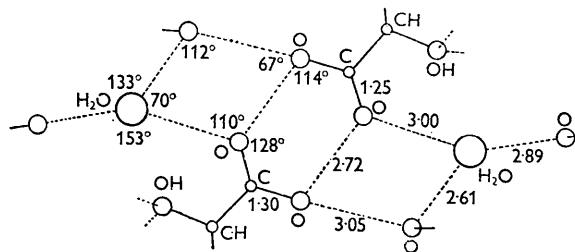


Fig. 13. The proposed arrangement of hydrogen bonds in the plane group containing the water molecule.

### References

- ALBRECHT, G. & COREY, R. B. (1939). *J. Amer. Chem. Soc.* **61**, 1087.  
 ASTBURY, W. T. (1923). *Proc. Roy. Soc. A*, **104**, 219.  
 BEEVERS, C. A. & HUGHES, W. (1941). *Proc. Roy. Soc. A*, **177**, 215.  
 BEEVERS, C. A. & STERN, F. (1948). *Nature, Lond.*, **162**, 854.  
 GERSTÄCKER, A., MÖLLER, H. & REIS, A. (1927). *Z. Kristallogr.* **66**, 421.  
 GOLDSCHMIDT, G. H. & PITT, G. J. (1948). *J. Sci. Instrum.* **25**, 397.  
 GROTH, P. (1906-19). *Chemische Kristallographie*. Leipzig: Engelmann.  
 HARKER, D. & KASPER, J. S. (1948). *Acta Cryst.* **1**, 70.  
 MORRISON, J. D. & ROBERTSON, J. M. (1949). *J. Chem. Soc.* p. 980.  
 PASTEUR, L. (1848). *Ann. Chim. (Phys.)*, **24**, 28.